Title

HAND2 targets define a network of transcriptional regulators that compartmentalize the early limb bud mesenchyme.

Permalink

Journal

Authors

Osterwalder, Marco
Speziale, Dario
Shoukry, Malak
et al.

Publication Date

DOI

Peer reviewed

HAND2 Targets Define a Network of Transcriptional Regulators that Compartmentalize the Early Limb Bud Mesenchyme

Marco Osterwalder[1], **Dario Speziale**[1], **Malak Shoukry**[2], **Rajiv Mohan**[3], **Robert Ivanek**[1], **Manuel Kohler**[4], **Christian Beisel**[4], **Xiaohui Wen**[5], **Suzie J. Scales**[5], **Vincent M. Christoffels**[3], **Axel Visel**[2,6,7], **Javier Lopez-Rios**[1,8], and **Rolf Zeller**[1,8]

[1]Developmental Genetics, Department Biomedicine, University of Basel, CH-4058 Basel, Switzerland [2]Genomics Division, MS 84-171, Lawrence Berkeley National Laboratory, Berkeley, CA 94720, USA [3]Department of Anatomy, Embryology, and Physiology, Heart Failure Research Center, Academic Medical Center, University of Amsterdam, 1100 DD Amsterdam, The Netherlands [4]Department for Biosystems Science and Engineering, Federal Institute of Technology Zurich, CH-4058 Basel, Switzerland [5]Department of Molecular Biology, Genentech, Inc., 1 DNA Way, South San Francisco, CA 94080, USA [6]U.S. Department of Energy Joint Genome Institute, Walnut Creek, CA 94598, USA [7]School of Natural Sciences, University of California, Merced, CA 95343, USA

Summary

The genetic networks that govern vertebrate development are well studied, but how the interactions of *trans*-acting factors with *cis*-regulatory modules (CRMs) are integrated into spatio-temporal regulation of gene expression is not clear. The transcriptional regulator HAND2 is required during limb, heart and branchial arch development. Here, we identify the genomic regions enriched in HAND2 chromatin complexes from mouse embryos and limb buds. Then, we analyze the HAND2 target CRMs in the genomic landscapes encoding transcriptional regulators required in early limb buds. HAND2 controls the expression of genes functioning in the proximal limb bud and orchestrates the establishment of anterior and posterior polarity of the nascent limb bud mesenchyme by impacting on *Gli3* and *Tbx3* expression. TBX3 is required downstream of HAND2 to refine the posterior *Gli3* expression boundary. Our analysis uncovers the transcriptional circuits that function in establishing distinct mesenchymal compartments downstream of HAND2 and upstream of SHH signaling.

---

[8]Co-corresponding authors: javier.lopez-rios@unibas.ch, rolf.zeller@unibas.ch.

Introduction

The limb bud is an excellent model to study the gene networks that govern growth and patterning during vertebrate organogenesis (Zeller et al., 2009). These gene regulatory networks impact on the expression of target genes via large *cis*-regulatory landscapes that integrate different inputs in a spatiotemporally controlled manner (Spitz and Furlong, 2012). For example, the expression of *Shh* in the posterior limb bud mesenchyme is controlled by a far upstream *cis*-regulatory module (CRM), termed ZRS (Lettice et al., 2003). Genetic ablation of the ZRS phenocopies the *Shh* loss-of function in mouse limb buds, which manifests itself in loss of digits (Sagai et al., 2005). In contrast, point mutations in the highly conserved core underlie pre-axial polydactyly in several species including humans (Anderson et al., 2012). Localized *Shh* expression depends on the interaction of different transcriptional regulators with the ZRS. In particular, the interaction with HOX, PBX, ETS and HAND2 transcriptional complexes has been implicated in activation of *Shh* in the limb bud, while TWIST1, ETV and GATA factors prevent anterior ectopic expression (Capellini et al., 2006; Galli et al., 2010; Kmita et al., 2005; Kozhemyakina et al., 2014; Lettice et al., 2014; Lettice et al., 2012; Mao et al., 2009; Zhang et al., 2010; Zhang et al., 2009). How the ZRS integrates these various inputs over time is unknown, but the resulting posterior restriction of SHH signaling is essential for proliferative expansion and anterior-posterior (AP) patterning of the distal limb bud mesenchyme that will form the skeletal elements of the zeugopod and autopod (Ahn and Joyner, 2004; Chiang et al., 2001; Harfe et al., 2004; Zhu et al., 2008).

The mesenchymal progenitors giving rise to the proximal-most skeletal structures (i.e. scapula and humerus in the forelimb) are likely specified prior to activation of SHH signaling (Ahn and Joyner, 2004; Dudley et al., 2002; Mariani et al., 2008; Mercader et al., 2000; Zeller et al., 2009). It has been shown that proximal mesenchymal progenitors express several transcriptional regulators belonging to the *Pbx*, *Meis* and *Irx* gene families, which participate in specification and/or morphogenesis of proximal skeletal elements (Capdevila et al., 1999; Capellini et al., 2010; Li et al., 2014; Mercader et al., 2000; Selleri et al., 2001). Genetic evidence indicates that *Raldh2*, which is involved in retinoic acid synthesis, regulates the expression of several of these early genes including the bHLH *Hand2* transcriptional regulator (Niederreither et al., 2002; Vitobello et al., 2011; Zhao et al., 2009).

Hand2 is genetically required for limb bud, branchial arch and heart development and the lethality of *Hand2*-deficient mouse embryos around embryonic day E9.5 is caused by the severe heart malformations (Srivastava et al., 1997; Vincentz et al., 2011). During early limb bud development, *Hand2* is required for AP polarization of the nascent limb bud mesenchyme and activation of *Shh* expression as part of its genetic interactions with *Gli3* (Charité et al., 2000; Galli et al., 2010). In particular, the *Hand2* and *Gli3* genetic antagonism is required to establish AP asymmetry and pentadactyly, as limb buds deficient for both these transcriptional regulators lack discernible AP polarity, *Shh* expression and are extremely polydactylous (Galli et al., 2010; te Welscher et al., 2002). As inactivation of *Hand2* after the onset of *Shh* expression does not severely alter limb bud development, *Hand2* functions are required mostly upstream of activating SHH signaling (Galli et al., 2010). However, the molecular nature of the underlying transcriptional and *cis*-regulatory

networks remained largely unknown, as *Shh* is the only known direct transcriptional target of HAND2 in limb buds.

We have inserted a 3xFLAG epitope-tag into the endogenous HAND2 protein to first determine the range of genomic regions enriched in endogenous HAND2 chromatin complexes. In a second step, we focused our in-depth analysis predominantly on HAND2 target genes that encode transcription factors expressed and/or required during early limb development. This analysis established that during the onset of limb bud outgrowth, HAND2 controls the expression of transcriptional regulators in the proximal mesenchyme that are involved in the formation of the proximal-most forelimb skeletal elements. In addition, our study reveals the gene regulatory logic by which HAND2, in cooperation with GLI3 and TBX3, establishes AP axis polarity in the early limb bud mesenchyme. In summary, our analysis uncovers the HAND2-dependent molecular circuits that function in establishing proximal, anterior and posterior compartments and activating *Shh* expression during the onset of limb bud development.

Results

A *Hand2*[3xFLAG] allele generated by dRMCE identifies the genomic regions enriched in endogenous HAND2 chromatin complexes

A 3xFLAG epitope tag was inserted into the endogenous HAND2 protein using dual recombinase-mediated cassette exchange (dRMCE, Osterwalder et al., 2010) to replace the conditional allele with a *Hand2*[3xFLAG] cassette in mouse ES-cells (Figure 1A and Supplemental Experimental Procedures). Insertion of the 3xFLAG epitope tag into the N-terminus does not alter HAND2 functions, as homozygous *Hand2*[3xFLAG] (*Hand2*[3xF/3xF]) mice develop normally and do not show any embryonic lethality (Galli et al., 2010; Srivastava et al., 1997 and data not shown). The 3xFLAG epitope tag allows sensitive detection of the endogenous HAND2 protein isoforms in embryonic tissues (limb buds, heart and branchial arches, Figure 1B and 1C). During the onset of forelimb bud outgrowth, HAND2-positive nuclei are detected in the posterior and proximal-anterior limb bud mesenchyme (green fluorescence, Figure 1D and Figure S1A, D) As HAND2 is required to activate *Shh* expression (Galli et al., 2010), we compared the distribution of HAND2-positive and *Shh*-expressing cells using the *Shh*-GFP allele (red fluorescence; Harfe et al., 2004). The *Shh*-expressing cells define a subdomain within the posterior HAND2-positive limb bud mesenchyme (Figure 1D and Figure S1D). We also co-localized HAND2 with the GLI3 repressor isoform (GLI3R) to determine their spatial distribution during activation of *Shh* expression. GLI3R proteins were detected by immunofluorescence using monoclonal GLI3 N-terminal antibodies (Wen et al., 2010) as they recognize the nuclear GLI3R isoform rather than the cytoplasmic full-length GLI3 and/or nuclear GLI3A activator isoforms in limb bud sections (Figure S1B-C). This analysis reveals the complementary distribution of the nuclear HAND2 (green) and GLI3R proteins (purple) in mouse forelimb bud mesenchymal cells (Figure 1D and Figure S1B-D).

The only known direct target of HAND2 in limb buds is *Shh*, whose transcriptional activation is controlled by interaction of HAND2 with the ZRS *cis*-regulatory region located ~850kb upstream of the *Shh* locus (Galli et al., 2010; Lettice et al., 2003). *Hand2*[3xF/3xF]

limb buds were used for chromatin immunoprecipitation using anti-FLAG antibodies in combination with quantitative real-time PCR (ChIP-qPCR). While our previous analysis did not unambiguously identify the HAND2-binding region(s) within the ZRS (Galli et al., 2010), ChIP of the endogenous HAND2[3xF] epitope tagged protein resulted in identification of a specific region within the ZRS (Figure 1E). Amplicon-tiling of the ZRS core (∼1.1 kb, Sagai et al., 2005) showed that a region encoding an *Ebox* is most enriched in HAND2 chromatin complexes (ZRS2-4 in Figure 1E, Dai and Cserjesi, 2002). This interaction is specific, as another *Ebox* sequence is not enriched (ZRS5, Figure 1E). The enrichment of the ZRS2-4 region in HAND2 chromatin complexes is highest in early limb buds (E10.5, Figure 1E) in agreement with the early but transient genetic requirement of *Hand2* for *Shh* activation (E10.5, Galli et al., 2010).

To define the range of potential HAND2 targets during its early genetic requirement in mouse limb buds, we used ChIP in combination with deep-sequencing (ChIP-Seq). To this aim, the HAND2 binding profile in all *Hand2* expressing embryonic tissues at E10.5 (eT, limb buds and flank tissue, hearts and branchial arches, Figure 1B) and dissected limb buds (Lb) was determined by HAND2[3xF] ChIP-Seq analysis (Figure 2A-D, Figure S2A). The primary datasets were analyzed using MACS-based peak calling and regions enriched in wild-type eT controls were excluded as non-specific (Table S1 and Table S2 list all statistically validated regions enriched   2 fold). For both validated ChIP-Seq datasets the top 1000 peaks were selected for the initial meta-analysis based on their fold-enrichment over the input control and number of reads (Figure 2A-D, Figure S2A and Tables S3 and S4). The majority of the top1000 HAND2-binding peaks in both datasets map to conserved sequences located   10kb away from the closest transcriptional start site (TSS, Figure 2A, 2B). *De novo* motif discovery showed that also the endogenous HAND2 chromatin complexes interact preferentially with the *Ebox* sequence defined *in vitro* (Figure 2C and Dai and Cserjesi, 2002).

Intersection of the top 1000 eT and Lb datasets shows that 259 of them are shared (Figure S2A and Table S5). GREAT analysis showed that the shared HAND2-binding regions are most often associated with genes known to function in limb bud and/or skeletal development (Figure 2D and Figure S2B). Hence, this set of shared regions and associated genes likely corresponds to HAND2 target genes in limb buds. However, it is important to consider that the sequence coverage was overall significantly lower for the Lb than the eT ChIP-Seq dataset. This is a likely consequence of the much lower amounts of tissue and HAND2 chromatin complexes recovered from the ∼1000 fine-dissected limb buds used for ChIP-Seq analysis (Supplemental Experimental Procedures). Furthermore the ZRS, which is an established HAND2 target region (Figure 1E) was moderately enriched only in the eT ChIP-Seq dataset (Table S4). This could reflect the fact that the HAND2-ZRS interaction occurs only in a small fraction of posterior mesenchymal cells in early limb buds and ChIP-qPCR analysis relying on specific oligos is more sensitive (Figure 1D and 1E). The limited sensitivity of in particular the Lb ChIP-Seq dataset indicates that not all relevant HAND2 binding peaks have been detected and represented in the top1000 peaks used for the comparative analysis. This is likely a consequence of a significant fraction of HAND2 target genes being restricted very proximally in early limb buds and extending into the flank

mesenchyme (see below). However, the flank mesenchyme was only included in the eT but not Lb ChIP-Seq sample. Therefore, all potential HAND2 target regions selected for further analysis were first verified in early limb buds (E10.5) using the more sensitive HAND2 ChIP-qPCR analysis (n=3, Experimental Procedures).

As we mainly wanted to get insight into the transcriptional circuitry controlled by HAND2 during pre-patterning of early limb buds (te Welscher et al., 2002), the current study focused on the genomic regions associated with transcription factors functioning and/or expressed upstream of activating *Shh* expression. To assess the expression of the associated genes in mutant mouse limb buds, *Hand2* was conditionally deleted during limb bud initiation using the *Hoxb6*-Cre transgene (Lowe et al., 2000). This inactivates *Hand2* in the posterior two thirds of the forelimb bud mesenchyme (Figure S2C-D), which results in almost complete penetrance of the *Hand2* loss-of-function limb bud phenotype (n=9/10). Our initial analysis of the curated list of genes expressed and/or functioning in early limb buds showed that most often their expression is altered in the posterior-proximal mesenchyme of *Hand2* $^{\Delta/\Delta c}$ forelimb buds (E10.25; n=17/29 genes analyzed, Table 1). Their expression is either significantly reduced or lost from the posterior mesenchyme (n=10/17; including *Ets1, Ets2, Gsc, Tbx2* and *Tbx3*; Table 1 and Figure S2E) or expands posteriorly (n= 7/17; including *Gli3, Tbx18, Irx3* and *Irx5*; Table 1 and Figure S2F). This initial analysis pointed to the existence of a network of transcriptional regulators that are direct targets of HAND2 during the onset of limb bud development (Table 1 and data not shown).

For example, two candidate CRMs located 23kb upstream of the *Ets1* and 146kb downstream of the *Ets2* TSS are significantly enriched in HAND2^{3xF} chromatin complexes as confirmed by ChIP-qPCR in early limb buds (Figure 2E and 2F). Indeed, the expression of both *Ets1* and *Ets2* is reduced in *Hand2*-deficient limb buds (Figure 2G). The *Ets2* +146kb CRM likely encodes an enhancer as the orthologous human region is active in the posterior limb bud mesenchyme of transgenic mouse embryos (left panel Figure 2H, Vista enhancer hs1516, Visel et al., 2007). The domain of the *LacZ* reporter not only recapitulates major aspects of *Ets2* expression (Figure 2H, middle panel) but also overlaps the endogenous *Hand2* domain (Figure 2H, right panel). These results establish the *Ets1* and *Ets2* genes as *bona fide* HAND2 target genes in early limb buds. As the *ETS* binding sites in the ZRS are essential for *Shh* expression in the posterior limb bud (Lettice et al, 2014; Lettice et al., 2012), HAND2-mediated up-regulation of the *Ets* transcription factors likely helps to reinforce *Shh* expression.

HAND2 target genes are required in the proximal limb bud for morphogenesis of the scapula and humerus

As part of the initial analysis, HAND2 peaks were detected in the genomic landscapes of several transcription factors expressed in the proximal limb bud mesenchyme (Figure 3 and Table 1) and that function in morphogenesis of proximal limb skeletal elements (scapula and humerus; Belo et al., 1998; Farin, 2009; Li et al., 2014). In particular, two prominent HAND2 peaks, whose enrichment in early limb buds was confirmed by ChIP-qPCR, map to the *Goosecoid (Gsc)* genomic landscape (at positions +33kb and -133kb; Figure 3A). *Gsc* is expressed in the proximal and flank mesenchyme during early limb bud development and is

required for scapular head development in the mouse (Belo et al., 1998). In agreement with *Gsc* being a direct transcriptional target of HAND2, its expression is lost from the posterior mesenchyme of *Hand2* ^{Δ/Δc} forelimb buds (Figure 3A). Genetic analysis underscores the functional importance of *Gsc* regulation by HAND2, as *Hand2* ^{Δ/Δc} and *Gsc*-deficient limbs display strikingly similar scapular defects affecting the glenoid cavity and coracoid process (n=4/8, Figure 3B, Figure S3A; compare to Belo et al., 1998). In limb buds, HAND2 chromatin complexes also interact with a specific region in the *Tbx18* genomic landscape (at position -338kb; middle panel, Figure 3C). Indeed, *Tbx18* expression expands posteriorly in *Hand2* ^{Δ/Δc} forelimb buds (Figure 3C) and previous genetic analysis established that *Tbx18* also functions during scapula and humerus development (Farin, 2009).

Recently, it has been shown that the *Irx3* and *Irx5* transcriptional regulators, which are part of the same gene cluster (Figure 3D) are required to specify the progenitors of proximal and anterior limb skeletal elements during limb bud initiation (Li et al., 2014). Interestingly, HAND2 chromatin complexes bind to a region located 85kb downstream of the *Irx3* TSS and adjacent to a GLI3R binding region (red bar in Figure 3D and Vokes et al., 2008). *Irx3* and *Irx5* are likely part of the same *cis*-regulatory landscape as they are co-expressed in the anterior-proximal limb bud mesenchyme and their expression expands posteriorly in *Hand2* ^{Δ/Δc} forelimb buds (Figure 3E). As this region encompasses binding regions for both HAND2 and GLI3R chromatin complexes, its enhancer potential (blue bar in Figure 3D) was assessed in transgenic mouse embryos (Figure 3F). Indeed, this region functions as a CRM in limb buds, but the mesenchymal *LacZ* reporter activity is rather uniform in contrast to the proximal-anterior restriction of the endogenous *Irx3* and *Irx5* expression domains (n=10/10, Figure 3F). Furthermore, as the GLI3R binding regions in limb buds (Vokes et al., 2008) often map close to the ones for HAND2 (red bars in Figure 3A, 3C, 3D, see also Figure S3B), the expression of these proximal genes was also analyzed in limb buds lacking both *Hand2* and *Gli3* (Figure S3C-D). While *Tbx18* expression is not significantly altered, the expression of *Gsc* and *Irx3* is much more reduced in double than wild-type or single mutant limb buds (Figure S3C-D and data not shown). These alterations in gene expression are paralleled by a more severely dysplastic scapula and humerus in *Hand2* ^{Δ/Δc}*Gli3* ^{Δ/Δ} limbs (Figure S3E). Together, these results indicate that HAND2 acts in concert with GLI3R to control a transcriptional network that functions in morphogenesis of proximal limb skeletal elements.

Direct cross-regulation between HAND2 and GLI3R underlies molecular establishment of an anterior and posterior limb bud compartment

Genetic analysis has shown that *Hand2* and *Gli3* are mutually antagonistic and this has been proposed to pre-pattern the limb bud mesenchyme along its AP axis prior to activation of SHH signaling (Galli et al., 2010; te Welscher et al., 2002). *Hand2* is initially expressed uniformly throughout the limb field mesenchyme, but its expression becomes rapidly posteriorly restricted as *Gli3* is activated in the anterior margin (Charité et al., 2000; te Welscher et al., 2002). At this early stage, the full-length cytoplasmic GLI3 protein is constitutively processed to GLI3R, which translocates to the nucleus in the absence of SHH signaling (Figure S4 and Wang et al., 2000). To gain insight into the underlying molecular and cellular interactions, we co-localized the endogenous HAND2^{3xF} and GLI3R proteins

during forelimb bud formation (E9.25, Figure 4A). HAND2 protein levels are highest in posterior and proximal-anterior nuclei (green fluorescence, Figure 4A), while GLI3R is most abundant in anterior nuclei (red fluorescence, Figure 4A). In spite of their opposing distribution, most mesenchymal cells co-express nuclear HAND2 and GLI3R proteins during forelimb bud formation (yellow overlap, n=4/4 at E9.25, Figure 4A and Figure S5A). Subsequently, HAND2 becomes undetectable in anterior cells, which retain GLI3R. Conversely, GLI3R is lost from posterior cell nuclei, which retain HAND2 (n=3/3 at E9.5-9.75, Figure 4B and Figure S5B). Cells at the interface of the two domains continue to co-express both proteins (Figures 4B and Figure S5B). These spatial dynamics reveal how the populations of GLI3R-positive anterior and HAND2-positive posterior cells segregate, likely concurrent with molecular establishment of AP axis polarity in forelimb buds. The SHH-independent nature of these interactions is revealed by the fact that the HAND2 and GLI3R domains are initially normal in *Shh*-deficient limb buds (E9.5-9.75, Figure S5C). During progression of forelimb bud outgrowth, the HAND2 and GLI3R domains are increasingly separated by cells expressing neither of these proteins (n=3/3 at E10.25, Figure 4B), which likely reflects the inhibition of GLI3R formation by SHH signaling. As the two proteins are initially co-expressed, direct cross-regulation could underlie establishment of the mutually exclusive HAND2 and GLI3R domains. Indeed, GLI3R interacts with two CRMs in the *Hand2* genomic landscape that function in repressing *Hand2* from the anterior limb bud mesenchyme (Vokes et al., 2008). The CRM at position +13kb is associated with one overlapping and a close-by region (at 11kb) enriched in HAND2 chromatin complexes from limb buds (Figure S5D-E). This indicates that in addition to mediating repression by GLI3R, this CRM could also participate in auto-regulation of *Hand2* expression.

As *Gli3* expression expands posteriorly in *Hand2*-deficient mouse limb buds (Galli et al., 2010; te Welscher et al., 2002), we screened also the *Gli3* genomic landscape for HAND2 interacting regions (Figure 4C). Indeed, a region located 120kb upstream of the *Gli3* transcription unit is prominently enriched in early limb buds (right panel, Figure 4C). Transgenic analysis showed that this CRM is indeed active both in fore- and hindlimb buds (Figure 4D). In particular, this CRM is able to drive *LacZ* expression in spatial pattern reminiscent of the endogenous *Gli3* transcript distribution, with *LacZ* being excluded from the posterior-most mesenchyme (n=6/7, Figure 4D and data not shown).

Tbx3 is a HAND2 target gene that positions the posterior *Gli3* expression boundary

HAND2 chromatin complexes are also enriched in two specific regions of the *Tbx3* genomic landscape that is required for expression in limb buds (Figure 5A, 5B and Horsthuis et al., 2009). While the eT and Lb HAND2 ChIP-Seq datasets do not unequivocally identify the two regions for the reasons stated above, HAND2 ChIP-qPCR using early limb buds established that the region located 58kb upstream of the *Tbx3* transcription unit is ~3-fold more enriched than the one located at -19kb (left panel Figure 5B). The enrichment of the *Tbx3* -58kb region is most prominent in early limb buds (right panel, Figure 5B), which points to an involvement of HAND2 in regulating the early *Tbx3* expression. This was corroborated by transgenic analysis, which established that the *Tbx3* -58kb CRM drives *LacZ* expression in the posterior-proximal forelimb bud and flank mesenchyme in a pattern strikingly similar to the endogenous *Tbx3* expression (n=8/10, Figure 5C and Figure S6A).

In contrast, the *Tbx3* -19kb region is not active in mouse limb buds (n=0/7, Figure S6A). The *Tbx3* -58kb CRM regulates *Tbx3* expression during early limb bud development, as the *LacZ* expression domain fails to expand distally as limb bud development progresses (Figure S6A). As neither of the two HAND2 binding regions is active in hindlimb buds (Figure 5C and data not shown), the expression of *Tbx3* in hindlimb buds must be controlled by different *cis*-regulatory interactions.

Indeed, *Tbx3* expression is lost from the posterior mesenchyme of *Hand2*-deficient forelimb buds, whilst it remains comparable to wild-types in mutant hindlimb buds (Figure 5D and Galli et al., 2010). Furthermore, the expression of *Tbx5*, which is located ∼163kb downstream of *Tbx3* as part of the same gene cluster, is not affected in *Hand2*-deficient forelimb buds (Figure S6B). Several HAND2 ChIP peaks were also detected in the *Tbx2-Tbx4* genomic landscape (Figure S6C-D). Similar to the *Tbx3-Tbx5* genomic landscape, *Tbx2* but not *Tbx4* expression is reduced in *Hand2*-deficient limb buds (Figure S6E-F). These apparent similarities in *cis*-regulation are likely related to the emergence of these gene clusters by duplication of an ancestral complex (Agulnik et al., 1996). Genetic and overexpression analysis has previously implicated *Tbx3* in early forelimb development together with *Hand2* and *Gli3* (Davenport et al., 2003; Rallis et al., 2005), while *Tbx2* is essential only during termination of limb bud outgrowth (Farin et al., 2013). Therefore, we focused our analysis on the HAND2-TBX3 interactions during the onset of forelimb bud development. HAND2 and TBX3 proteins are initially co-expressed (Figure S6G). However, TBX3 becomes rapidly more restricted than HAND2 such that the double-positive cells hallmark the proximal-posterior forelimb bud and posterior flank (Figure 5E). In *Shh*-deficient forelimb buds both protein domains are more restricted but otherwise maintained (right panel, Figure 5D). In contrast, TBX3 is absent from *Hand2* $^{\Delta/\Delta c}$ and *Hand2* $^{\Delta/\Delta c}$*Gli3* $^{\Delta/\Delta}$ forelimb buds with exception of few positive cells at the proximal border (right panels, Figure 5F). Taken together, these results provide compelling evidence that *Tbx3* is a direct transcriptional target of HAND2 in the posterior and flank mesenchyme during the onset of limb bud development.

To gain insight into the potential involvement of TBX3 in AP patterning of the early limb bud mesenchyme, the spatial distribution of the mesenchymal cells actively transcribing *Gli3* was determined in relation to HAND2 and TBX3 proteins (Figure 6A, 6B). To achieve cellular resolution, the *Gli3* allele expressing EGFP under control of the endogenous locus (Lopez-Rios et al., 2012) was used in combination with GFP antibodies (red fluorescence; Figure 6A, 6B). While the GLI3R and HAND2 protein domains are increasingly separated (Figure 4B), a significant fraction of boundary cells continue to co-express HAND2 protein and *Gli3* transcripts in wild-type limb buds (yellow fluorescence, left panels Figure 6A). In contrast, far fewer cells co-express TBX3 and *Gli3* in the boundary region (right panels Figure 6A). This difference is even more striking in *Gli3* $^{\Delta/\Delta}$ forelimb buds, which continue to express the mutant *Gli3* transcripts (Figure 6B). There is a large population of cells co-expressing HAND2 and *Gli3* due to the anterior expansion of the *Hand2* expression domain in *Gli3*-deficient limb buds (left panels Figure 6B and te Welscher et al., 2002). However, TBX3 remains posteriorly restricted in *Gli3*-deficient limb buds and, similar to wild-types, only few cells co-express TBX3 proteins and *Gli3* transcripts (right panels Figure 6B). This

boundary is also retained in *Shh*-deficient forelimb buds in spite of the posterior expansion of *Gli3* (Figure S7A,B). These results show that HAND2 is not sufficient to establish a sharp boundary, but rather that TBX3 defines the limit between the anterior *Gli3*-positive and posterior *Gli3*-negative mesenchymal cells. Indeed, the comparative analysis of wild-type, *Shh*- and *Tbx3*-deficient forelimb buds reveals that *Tbx3* is required to establish this boundary (Figure 6C, 6D). In *Shh*-deficient limb buds, *Gli3* transcription expands posteriorly with more restricted HAND2 and TBX3 domains, but fails to reach the posterior margin (right panel, Figure 6C, Figure 5E and Figure S7A). Rather strikingly, *Gli3* expression expands into the posterior flank mesenchyme in *Tbx3*-deficient forelimb buds as in *Hand2*-deficient limb buds (Figure 6D). *Hand2*-deficient forelimb buds lack *Tbx3* (Figure 5D and 5F) in their posterior mesenchyme, while *Hand2* transcripts remain in *Tbx3*-deficient limb buds albeit at reduced levels (Figure S7C). Together, these results corroborate the proposal that the HAND2 transcriptional target *Tbx3* is required to establish the posterior *Gli3* expression boundary by inhibiting its expression in the posterior-most mesenchyme (Figure 6, 7).

Discussion

There is ample evidence that tissue-specific CRMs orchestrate the dynamics of gene expression during embryonic development and fine-tune morphogenesis as a consequence of their often highly dynamic regulation (Attanasio et al., 2013; Spitz and Furlong, 2012). Functional modification of CRMs in an increasing number of genomic landscapes have been causally linked to both adaptive evolution and human congenital malformations (Anderson et al., 2012; Lopez-Rios et al., 2014). Therefore it is important to identify the *trans*-acting factors and complexes that regulate these CRMs in a tissue and stage-specific manner. To this aim, we have inserted a 3xFLAG-tag into the endogenous HAND2 protein, which permitted us to uncover genomic regions enriched in HAND2-containing chromatin complexes in mouse embryos. The current study focuses on an in-depth functional analysis of HAND2-CRMs in genomic landscapes of transcriptional regulators that are required during early mouse forelimb bud development. This analysis uncovers the architecture of a network of HAND2 target transcription factors that function in early determinative events that set up the proximal, anterior and posterior domains during the onset of forelimb bud outgrowth (Figure 7). An essential role of HAND2 in proximal skeletal development was revealed by the fact that its early *Hoxb6*-Cre mediated conditional inactivation disrupts scapular head morphogenesis. Our study provides good evidence that this is a consequence of HAND2 directly regulating the expression of transcription factors that function in the development of the proximal limb skeletal elements such as *Gsc*, *Irx3*, *Irx5* and *Tbx18* (Figure 7). In particular, the HAND2 ChIP analysis identifies a CRM located upstream of *Irx3* that is active in the limb bud mesenchyme. In turn, IRX3 regulates *Gli3* expression by directly interacting with a limb bud mesenchymal CRM located in the *Gli3* genomic landscape (Abbasi et al., 2010; Li et al., 2014). These direct interactions begin to reveal the underlying complexity of the *cis*-regulatory circuitry operating during the onset of limb bud development (Figure 7). In summary, our genetic analysis supports the proposal that the HAND2-regulated gene networks are required to pattern the early mesenchymal territory

that gives rise to the proximal limb skeletal elements in a *Shh*-independent manner (Ahn and Joyner, 2004; Chiang et al., 2001).

It is unclear at what stage AP axis polarity is established in mouse limb buds, but Tanaka and coworkers (Tanaka et al., 2000) showed that the competence to activate *Shh* expression is widespread and without posterior bias in the forelimb field of early mouse embryos (E9.0). Together with other studies (see Introduction), this suggests that the limb bud mesenchyme might only be polarized along the AP axis during the onset of limb bud development in mouse embryos. The present study shows that the nuclear HAND2 and GLI3R proteins are initially co-expressed by the mesenchymal progenitors that give rise to the forelimb bud. However during initiation of limb bud development, the spatial distributions of the two transcriptional regulators rapidly segregates into a distinct GLI3R-positive anterior and HAND2-positive posterior compartment. In addition to establishing this dynamic segregation with cellular resolution, we identify the HAND2-dependent *cis*-regulatory interactions and transcription factor networks that establish these anterior and posterior compartments (Figure 7). The loss of *Hand2* transcripts and proteins from the anterior limb bud mesenchyme (te Welscher et al., 2002 and this study) is the result of GLI3R-mediated direct repression (Vokes et al., 2008). The HAND2 ChIP analysis identifies one CRM in the *Gli3* genomic landscape that is active in limb buds with exception of the most posterior mesenchyme. The transcriptional regulation of *Gli3* in early limb buds is complex and likely controlled by several CRMs with similar activities, one of which is bound by IRX3, a direct transcriptional target of *Hand2* (Abbasi et al., 2010; Li et al., 2014; Visel et al., 2007 and this study). While the genetic analysis shows that *Hand2* is required to repress the expression of *Gli3* and other direct targets in the posterior mesenchyme, our transgenic studies of HAND2-interacting CRMs rather reveals their ability to activate *LacZ* expression in the limb bud mesenchyme. HAND2 was first described as a transcriptional activator (Dai and Cserjesi, 2002), but more recently its transcriptional repressing activity has been established in the context of its interaction with a specific CRM that regulates the *Dlx5/6* gene cluster (Barron et al., 2011). Furthermore, HAND2 forms heterodimers with transcriptional repressors such as TWIST1 and RUNX2 (Firulli et al., 2005; Funato et al., 2009), which could determine the repressive activity of HAND2 chromatin complexes interacting with CRMs in e.g. the *Gli3* genomic landscape. Alternatively, the repressive effect of HAND2 on *Gli3* could be mediated via the transcriptional target *Tbx3*, which is required to repress *Gli3* in the posterior mesenchyme. In fact, TBX3 has an essential role in positioning the *Gli3* expression boundary (Figure 7) and its overexpression in forelimb buds of chicken embryos inhibits *Gli3* expression (Rallis et al., 2005). Finally, HAND2 controls the activation of *Shh* expression by directly binding to the ZRS and indirectly via its transcriptional targets *Ets1* and *Ets2* that also regulate *Shh* (Lettice et al., 2014; Lettice et al., 2012). Such feed-forward loops are important motifs within transcriptional networks as they contribute to their stability and robustness (Alon, 2007).

Previous studies had provided genetic and experimental evidence that both proximo-distal and AP identities are specified early during limb bud development (Dudley et al., 2002; Zhu et al., 2008). Our study now uncovers distinct transcriptional networks interlinked by HAND2 that are required to setup the initial proximal, posterior and anterior mesenchymal

compartments prior to the onset of SHH signaling. These networks define proximal fates and the AP boundaries with cellular precision through selective activation and/or repression of downstream transcriptional regulators. The direct cross-regulation among these transcriptional regulators not only defines the limb bud mesenchymal compartments, but also enables activation of SHH signaling, which then elaborates these compartments during distal progression of limb bud outgrowth.

Experimental Procedures

For generation of the *Hand2*^{3xF} allele and details on methodology see Supplemental Experimental Procedures.

Mouse strains and embryos

Experiments involving mice were performed strictly adhering to Swiss law, the 3R principles and the Basel Declaration. All animal studies were approved by the cantonal animal welfare and ethics committees. The procedures for generating transgenic mice at the Lawrence Berkeley National Laboratory (LBNL) were reviewed and approved by the LBNL Animal Welfare and Research Committee. The *Hand2*^{3xF} and *Gli3*^{C3xF} alleles were maintained in an NMRI background. The *Hand2*^{f} (floxed), *Hand2*^{Δ} and *Gli3*^{ΔGFP} alleles were maintained in mixed backgrounds. The *Gli3*^{C3xF} allele was constructed by inserting a 3XFLAG epitope tag in frame at the carboxy-terminus of the endogenous GLI3 protein. Western blotting detects the 190kD full-length GLI3 protein. Mice and embryos homozygous for this allele are phenotypically wild-type and will be described elsewhere (J. Lopez-Rios and R. Zeller, unpublished). The *Shh*^{GFPCre} allele (Harfe et al., 2004) and the *Hoxb6-Cre* transgene (Lowe et al., 2000) were maintained in a C57BL/6J background. The *Tbx3*^{Venus} allele used to generate *Tbx3*-deficient embryos recapitulates all known *Tbx3* loss-of-function phenotypes and will be described elsewhere (R. Mohan and V. Christoffels, unpublished).

Immunofluorescence

Limb buds were fixed in 4% paraformaldehyde for 2-3 hours at 4°C and proteins were detected on 10μm cryosections. Primary antibodies against the FLAG epitope (M2; 1:500; Sigma), GLI3 (3.6ng/ml; clone 6F5; Wen et al., 2010), TBX3 (1:300; E-20; Santa Cruz) and GFP (1:1000; Life Technologies) were used. Goat anti-mouse (FLAG/GLI3), goat anti-rabbit (GFP), rabbit/donkey anti-goat (TBX3) secondary antibodies conjugated to Alexa Fluor 488 or 594 (1:1000; Life Technologies) were used for detection. For co-localization of HAND2 and GLI3R, anti-FLAG (M2; F3165, Sigma) antibodies were labeled with Alexa Fluor 488 using the APEX antibody labeling kit (Life Technologies). Sequential treatment with rabbit anti-Alexa Fluor 488 (Life Technologies) and goat anti-rabbit 488 Alexa Fluor enhanced the signal. Nuclei were counterstained with Hoechst-33258. The *Shh*^{GFPCre} and *Gli3*^{ΔGFP} null alleles were used in combination with immunodetection of GFP to visualize cells expressing *Shh* or *Gli3*, respectively. The autofluorescence of e.g. blood cells was detected equally in all channels. Therefore, it was captured utilizing the 633nm laser of the confocal microscope and digitally removed using the subtraction mode in Photoshop CS5

Author Manuscript

Author Manuscript

Author Manuscript

Author Manuscript

(Adobe) as shown in Figure S1A. Images were acquired using a Leica SP5 confocal microscope.

ChIP-qPCR and ChIP-Seq analysis

Fore- and hindlimb buds dissected from ∼50 *Hand2*$^{3xF/3xF}$ embryos at E10.5 were processed for ChIP as described (Lopez-Rios et al, 2012; Vokes et al., 2008) using M2 anti-FLAG antibody (F1804, Sigma). For time-course experiments, 20 fore- and hindlimbs of E11.5 or E12.5 *Hand2*$^{3xF/3xF}$ embryos were processed in an identical manner. Chromatin was fragmented for 15min (E10.5) or 20min (E11.5, E12.5) using a S220 Covaris Ultra-sonicator, which yielded average fragment sizes in the range of 200-300bp. All results (mean±SD) represent 3 independent biological replicates. The details of the ChIP-Seq analysis are given in the Supplemental Experimental Procedures and all datasets have been deposited in the GEO database under the accession number GSE55707.

Supplementary Material

Refer to Web version on PubMed Central for supplementary material.

Acknowledgments

References

Abbasi AA, Paparidis Z, Malik S, Bangs F, Schmidt A, Koch S, Lopez-Rios J, Grzeschik KH. Human intronic enhancers control distinct sub-domains of Gli3 expression during mouse CNS and limb development. BMC Dev Biol. 2010; 10:44. [PubMed: 20426846]

Agulnik SI, Garvey N, Hancock S, Ruvinsky I, Chapman DL, Agulnik I, Bollag R, Papaioannou V, Silver LM. Evolution of mouse T-box genes by tandem duplication and cluster dispersion. Genetics. 1996; 144:249–254. [PubMed: 8878690]

Ahn S, Joyner AL. Dynamic changes in the response of cells to positive hedgehog signaling during mouse limb patterning. Cell. 2004; 118:505–516. [PubMed: 15315762]

Alon U. Network motifs: theory and experimental approaches. Nat Rev Genet. 2007; 8:450–461. [PubMed: 17510665]

Anderson E, Peluso S, Lettice LA, Hill RE. Human limb abnormalities caused by disruption of hedgehog signaling. Trends Genet. 2012; 28:364–373. [PubMed: 22534646]

Attanasio C, Nord AS, Zhu Y, Blow MJ, Li Z, Liberton DK, Morrison H, Plajzer-Frick I, Holt A, Hosseini R, et al. Fine tuning of craniofacial morphology by distant-acting enhancers. Science. 2013; 342:1241006. [PubMed: 24159046]

Barron F, Woods C, Kuhn K, Bishop J, Howard MJ, Clouthier DE. Downregulation of Dlx5 and Dlx6 expression by Hand2 is essential for initiation of tongue morphogenesis. Development. 2011; 138:2249–2259. [PubMed: 21558373]

Belo JA, Leyns L, Yamada G, De Robertis EM. The prechordal midline of the chondrocranium is defective in Goosecoid-1 mouse mutants. Mech Dev. 1998; 72:15–25. [PubMed: 9533949]

Capdevila J, Tsukui T, Rodriquez Esteban C, Zappavigna V, Izpisua Belmonte JC. Control of vertebrate limb outgrowth by the proximal factor Meis2 and distal antagonism of BMPs by Gremlin. Mol Cell. 1999; 4:839–849. [PubMed: 10619030]

Capellini TD, Di Giacomo G, Salsi V, Brendolan A, Ferretti E, Srivastava D, Zappavigna V, Selleri L. Pbx1/Pbx2 requirement for distal limb patterning is mediated by the hierarchical control of Hox gene spatial distribution and Shh expression. Development. 2006; 133:2263–2273. [PubMed: 16672333]

Capellini TD, Vaccari G, Ferretti E, Fantini S, He M, Pellegrini M, Quintana L, Di Giacomo G, Sharpe J, Selleri L, et al. Scapula development is governed by genetic interactions of Pbx1 with its family members and with Emx2 via their cooperative control of Alx1. Development. 2010; 137:2559–2569. [PubMed: 20627960]

Charité J, McFadden DG, Olson EN. The bHLH transcription factor dHAND controls *Sonic hedgehog* expression and establishment of the zone of polarizing activity during limb development. Development. 2000; 127:2461–2470. [PubMed: 10804186]

Chiang C, Litingtung Y, Harris MP, Simandl BK, Li Y, Beachy PA, Fallon JF. Manifestation of the limb prepattern: limb development in the absence of sonic hedgehog function. Dev Biol. 2001; 236:421–435. [PubMed: 11476582]

Cotney J, Leng J, Oh S, DeMare LE, Reilly SK, Gerstein MB, Noonan JP. Chromatin state signatures associated with tissue-specific gene expression and enhancer activity in the embryonic limb. Genome Res. 2012; 22:1069–1080. [PubMed: 22421546]

Dai YS, Cserjesi P. The basic helix-loop-helix factor, HAND2, functions as a transcriptional activator by binding to E-boxes as a heterodimer. J Biol Chem. 2002; 277:12604–12612. [PubMed: 11812799]

Davenport TG, Jerome-Majewska LA, Papaioannou VE. Mammary gland, limb and yolk sac defects in mice lacking Tbx3, the gene mutated in human ulnar mammary syndrome. Development. 2003; 130:2263–2273. [PubMed: 12668638]

Dudley AT, Ros MA, Tabin CJ. A re-examination of proximodistal patterning during vertebrate limb development. Nature. 2002; 418:539–544. [PubMed: 12152081]

Farin, H. PhD Thesis. University of Hannover; 2009. Function and regulation of the murine T-box genes Tbx15 and Tbx18.

Farin HF, Ludtke TH, Schmidt MK, Placzko S, Schuster-Gossler K, Petry M, Christoffels VM, Kispert A. Tbx2 terminates shh/fgf signaling in the developing mouse limb bud by direct repression of gremlin1. PLoS Genet. 2013; 9:e1003467. [PubMed: 23633963]

Firulli BA, Krawchuk D, Centonze VE, Vargesson N, Virshup DM, Conway SJ, Cserjesi P, Laufer E, Firulli AB. Altered Twist1 and Hand2 dimerization is associated with Saethre-Chotzen syndrome and limb abnormalities. Nat Genet. 2005; 37:373–381. [PubMed: 15735646]

Funato N, Chapman SL, McKee MD, Funato H, Morris JA, Shelton JM, Richardson JA, Yanagisawa H. Hand2 controls osteoblast differentiation in the branchial arch by inhibiting DNA binding of Runx2. Development. 2009; 136:615–625. [PubMed: 19144722]

Galli A, Robay D, Osterwalder M, Bao X, Benazet JD, Tariq M, Paro R, Mackem S, Zeller R. Distinct roles of Hand2 in initiating polarity and posterior Shh expression during the onset of mouse limb bud development. PLoS Genet. 2010; 6:e1000901. [PubMed: 20386744]

Harfe BD, Scherz PJ, Nissim S, Tian H, McMahon AP, Tabin CJ. Evidence for an expansion-based temporal Shh gradient in specifying vertebrate digit identities. Cell. 2004; 118:517–528. [PubMed: 15315763]

Horsthuis T, Buermans HP, Brons JF, Verkerk AO, Bakker ML, Wakker V, Clout DE, Moorman AF, t Hoen PA, Christoffels VM. Gene expression profiling of the forming atrioventricular node using a novel tbx3-based node-specific transgenic reporter. Circ Res. 2009; 105:61–69. [PubMed: 19498200]

Kmita M, Tarchini B, Zakany J, Logan M, Tabin CJ, Duboule D. Early developmental arrest of mammalian limbs lacking HoxA/HoxD gene function. Nature. 2005; 435:1113–1116. [PubMed: 15973411]

Kozhemyakina E, Ionescu A, Lassar AB. GATA6 is a crucial regulator of Shh in the limb bud. PLoS Genet. 2014; 10:e1004072. [PubMed: 24415953]

Lettice LA, Heaney SJ, Purdie LA, Li L, de Beer P, Oostra BA, Goode D, Elgar G, Hill RE, de Graaff E. A long-range Shh enhancer regulates expression in the developing limb and fin and is associated with preaxial polydactyly. Hum Mol Genet. 2003; 12:1725–1735. [PubMed: 12837695]

Lettice LA, Williamson I, Devenney PS, Kilanowski F, Dorin J, Hill RE. Development of five digits is controlled by a bipartite long-range cis-regulator. Development. 2014; 141:1715–1725. [PubMed: 24715461]

Lettice LA, Williamson I, Wiltshire JH, Peluso S, Devenney PS, Hill AE, Essafi A, Hagman J, Mort R, Grimes G, et al. Opposing Functions of the ETS Factor Family Define Shh Spatial Expression in Limb Buds and Underlie Polydactyly. Dev Cell. 2012; 22:459–467. [PubMed: 22340503]

Li D, Sakuma R, Vakili NA, Mo R, Puviindran V, Deimling S, Zhang X, Hopyan S, Hui CC. Formation of proximal and anterior limb skeleton requires early function of Irx3 and Irx5 and is negatively regulated by Shh signaling. Dev Cell. 2014; 29:233–240. [PubMed: 24726282]

Lopez-Rios J, Duchesne A, Speziale D, Andrey G, Peterson KA, Germann P, Unal E, Liu J, Floriot S, Barbey S, et al. Attenuated sensing of SHH by Ptch1 underlies evolution of bovine limbs. Nature. 2014; 511:46–51. [PubMed: 24990743]

Lopez-Rios J, Speziale D, Robay D, Scotti M, Osterwalder M, Nusspaumer G, Galli A, Holländer GA, Kmita M, Zeller R. GLI3 Constrains Digit Number by Controlling Both Progenitor Proliferation and BMP-Dependent Exit to Chondrogenesis. Dev Cell. 2012; 22:837–848. [PubMed: 22465667]

Lowe LA, Yamada S, Kuehn MR. HoxB6-Cre transgenic mice express Cre recombinase in extra-embryonic mesoderm, in lateral plate and limb mesoderm and at the midbrain/hindbrain junction. Genesis. 2000; 26:118–120. [PubMed: 10686603]

Mao J, McGlinn E, Huang P, Tabin CJ, McMahon AP. Fgf-dependent Etv4/5 activity is required for posterior restriction of Sonic Hedgehog and promoting outgrowth of the vertebrate limb. Dev Cell. 2009; 16:600–606. [PubMed: 19386268]

Mariani FV, Ahn CP, Martin GR. Genetic evidence that FGFs have an instructive role in limb proximal-distal patterning. Nature. 2008; 453:401–405. [PubMed: 18449196]

Mercader N, Leonardo E, Piedra ME, Martinez AC, Ros MA, Torres M. Opposing RA and FGF signals control proximodistal vertebrate limb development through regulation of Meis genes. Development. 2000; 127:3961–3970. [PubMed: 10952894]

Niederreither K, Vermot J, Schuhbaur B, Chambon P, Dolle P. Embryonic retinoic acid synthesis is required for forelimb growth and anteroposterior patterning in the mouse. Development. 2002; 129:3563–3574. [PubMed: 12117807]

Osterwalder M, Galli A, Rosen B, Skarnes WC, Zeller R, Lopez-Rios J. Dual RMCE for efficient re-engineering of mouse mutant alleles. Nat Meth. 2010; 7:893–895.

Rallis C, Del Buono J, Logan MP. Tbx3 can alter limb position along the rostrocaudal axis of the developing embryo. Development. 2005; 132:1961–1970. [PubMed: 15790970]

Sagai T, Hosoya M, Mizushina Y, Tamura M, Shiroishi T. Elimination of a long-range cis-regulatory module causes complete loss of limb-specific Shh expression and truncation of the mouse limb. Development. 2005; 132:797–803. [PubMed: 15677727]

Selleri L, Depew MJ, Jacobs Y, Chanda SK, Tsang KY, Cheah KS, Rubenstein JL, O'Gorman S, Cleary ML. Requirement for Pbx1 in skeletal patterning and programming chondrocyte proliferation and differentiation. Development. 2001; 128:3543–3557. [PubMed: 11566859]

Spitz F, Furlong EE. Transcription factors: from enhancer binding to developmental control. Nat Rev Genet. 2012; 13:613–626. [PubMed: 22868264]

Srivastava D, Thomas T, Lin Q, Kirby ML, Brown D, Olson EN. Regulation of cardiac mesodermal and neural crest development by the bHLH transcription factor, dHAND. Nat Genet. 1997; 16:154–160. [PubMed: 9171826]

Tanaka M, Cohn MJ, Ashby P, Davey M, Martin P, Tickle C. Distribution of polarizing activity and potential for limb formation in mouse and chick embryos and possible relationships to polydactyly. Development. 2000; 127:4011–4021. [PubMed: 10952899]

te Welscher P, Fernandez-Teran M, Ros MA, Zeller R. Mutual genetic antagonism involving GLI3 and dHAND prepatterns the vertebrate limb bud mesenchyme prior to SHH signaling. Genes Dev. 2002; 16:421–426. [PubMed: 11850405]

Vincentz JW, Barnes RM, Firulli AB. Hand factors as regulators of cardiac morphogenesis and implications for congenital heart defects. Birth Defects Res Part A, Clin Mol Terat. 2011; 91:485–494.

Visel A, Minovitsky S, Dubchak I, Pennacchio LA. VISTA Enhancer Browser--a database of tissue-specific human enhancers. Nucl Acids Res. 2007; 35:D88–92. [PubMed: 17130149]

Vitobello A, Ferretti E, Lampe X, Vilain N, Ducret S, Ori M, Spetz JF, Selleri L, Rijli FM. Hox and Pbx factors control retinoic acid synthesis during hindbrain segmentation. Dev Cell. 2011; 20:469–482. [PubMed: 21497760]

Vokes SA, Ji H, Wong WH, McMahon AP. A genome-scale analysis of the cis-regulatory circuitry underlying sonic hedgehog-mediated patterning of the mammalian limb. Genes Dev. 2008; 22:2651–2663. [PubMed: 18832070]

Wang B, Fallon JF, Beachy PA. Hedgehog-regulated processing of Gli3 produces an anterior/posterior repressor gradient in the developing vertebrate limb. Cell. 2000; 100:423–434. [PubMed: 10693759]

Wen X, Lai CK, Evangelista M, Hongo JA, de Sauvage FJ, Scales SJ. Kinetics of hedgehog-dependent full-length Gli3 accumulation in primary cilia and subsequent degradation. Mol Cell Biol. 2010; 30:1910–1922. [PubMed: 20154143]

Zeller R, Lopez-Rios J, Zuniga A. Vertebrate limb bud development: moving towards integrative analysis of organogenesis. Nat Rev Genet. 2009; 10:845–858. [PubMed: 19920852]

Zhang Z, Sui P, Dong A, Hassell J, Cserjesi P, Chen YT, Behringer RR, Sun X. Preaxial polydactyly: interactions among ETV, TWIST1 and HAND2 control anterior-posterior patterning of the limb. Development. 2010; 137:3417–3426. [PubMed: 20826535]

Zhang Z, Verheyden JM, Hassell JA, Sun X. FGF-regulated Etv genes are essential for repressing Shh expression in mouse limb buds. Dev Cell. 2009; 16:607–613. [PubMed: 19386269]

Zhao X, Sirbu IO, Mic FA, Molotkova N, Molotkov A, Kumar S, Duester G. Retinoic acid promotes limb induction through effects on body axis extension but is unnecessary for limb patterning. Curr Biol. 2009; 19:1050–1057. [PubMed: 19464179]

Zhu J, Nakamura E, Nguyen MT, Bao X, Akiyama H, Mackem S. Uncoupling Sonic hedgehog control of pattern and expansion of the developing limb bud. Dev Cell. 2008; 14:624–632. [PubMed: 18410737]
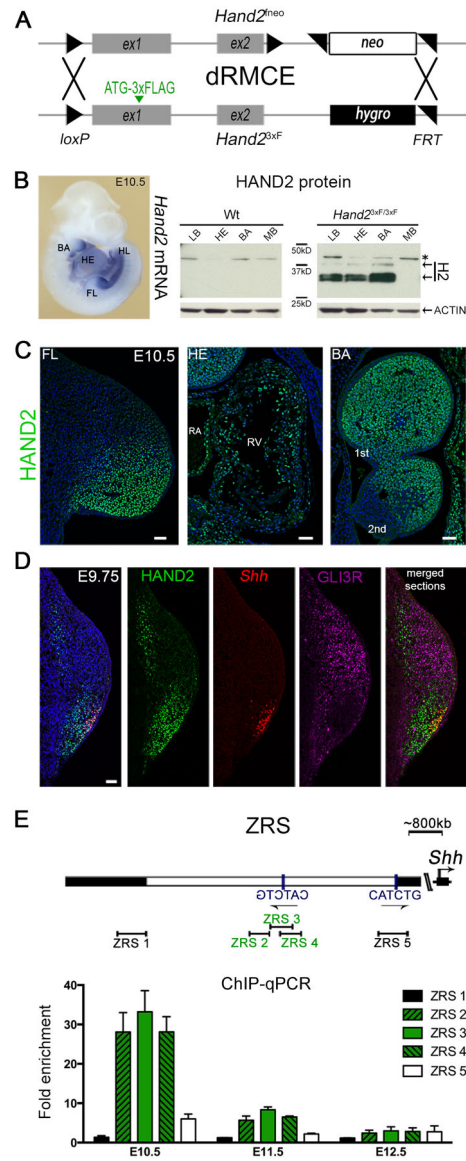
Figure 1. Insertion of a 3xFLAG epitope tag into the endogenous HAND2 protein provides a sensitive tool to detect HAND2 protein complexes

(A) The *Hand2*[3xF] allele was generated by dRMCE in mouse ES cells.

(B) Left panel: *Hand2* expressing tissues in mouse embryos at embryonic dayE10.5. Right panels: immunoblot detection of the tagged HAND2[3xF] protein isoforms (H2) in limb buds (LB), heart (HE) and branchial arches (BA). Midbrain (MB) and wild-type extracts are used as negative controls. Anasterisk indicates a non-specific band. FL: forelimb bud. HL: hindlimb bud.

(C) Detection of HAND2[3xF] proteins in expressing embryonic tissues by immunofluorescence (green) at E10.5. RV: right ventricle; RA: right atrium.1st: mandibular arch. 2nd: hyoid arch.

(D) Co-localization of HAND2[3xF] proteins (green) and *Shh* transcripts (red) in limb buds (E9.75, 28-29 somites). The distribution of nuclear GLI3R proteins(magenta) is shown on an adjacent section. The right-most panel shows an artificial overlap of the two consecutive

sections. Limb buds are always oriented with anterior to the top and posterior to the bottom. Nuclei are blue due to counterstaining with Hoechst. Scale bars: 50μm.

(E) ChIP-qPCR analysis shows the interaction of HAND2[3xF] chromatin complexes with a specific region in the ZRS in developing limb buds (E10.5, E11.5 and E12.5). The *Ebox* core sequence (CATCTG) defined by *in vitro* analysis is indicated. The most relevant qPCR amplicons used are indicated as ZRS 1 - ZRS 5. Fold-enrichment is shown as mean ±SD (n=3). See also Figure S1.
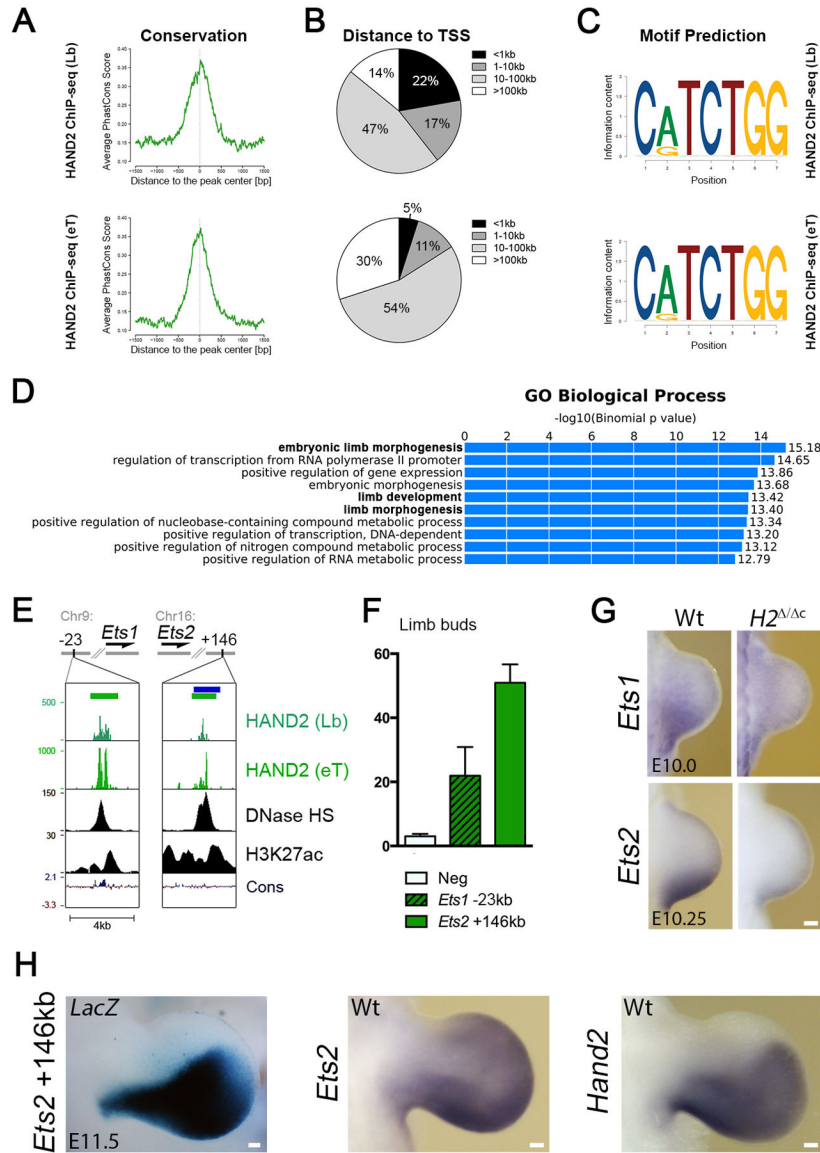
Figure 2. ChIP-Seq analysis identifies a set of HAND2 target regions in mouse limb buds

(A, B) The top 1000 HAND2[3xF] target regions enriched in E10.5 limb buds (Lb) and *Hand2* expressing embryonic tissues (eT) are mostly evolutionarily conserved (panel A) and map generally 10kb away from the closest transcriptional start site (TSS, panel B).

(C) *De novo* motif discovery analysis of the top 1000 HAND2[3xF] bound regions reveals enrichment in *Ebox* consensus sequences.

(D) Gene ontology (GO) analysis reveals the most prominent biological processes associated with HAND2[3xF] binding regions that are represented in both top 1000 Lb and eT datasets.

(E) UCSC Genome Browser window shows the *Ets1* and *Ets2* regions enriched in HAND2 chromatin complexes from limb buds (Lb) and expressing tissues (eT). Distances to the *Ets1 and Ets2* TSS are indicated in kb. The profiles of DNaseI HS and H3K27ac marks in limb buds (E11.5) are shown in black (Cotney et al., 2012). The placental mammal conservation (Cons) plot(PhyloP) is shown below. Green bars represent the peaks identified by MACS

analysis. The blue bar indicates the hs1516 enhancer element assayed by *LacZ* transgenesis (Vista Enhancer Browser). The ChIP-Seq panels in all figures are organized the same.

(F) ChIP-qPCR statistically verifies the HAND2^{3xF} binding regions in the *Ets1* and *Ets2* genomic landscapes in limb buds (n=3; E10.5). Mean ±SD is shown.

(G) *Ets1* and *Ets2* transcript distribution in wild-type and *Hand2* $^{/ c}$ forelimb buds (E10.25).

(H) The activity of the *Ets2* +146kb human orthologue (hs1516-*LacZ* reporter, Vista Enhancer Browser) is compared with the endogenous *Ets2* and *Hand2* expression in forelimb buds (E11.5). Scale bars: 100μm. See also Figure S2 and Tables S1-S5.
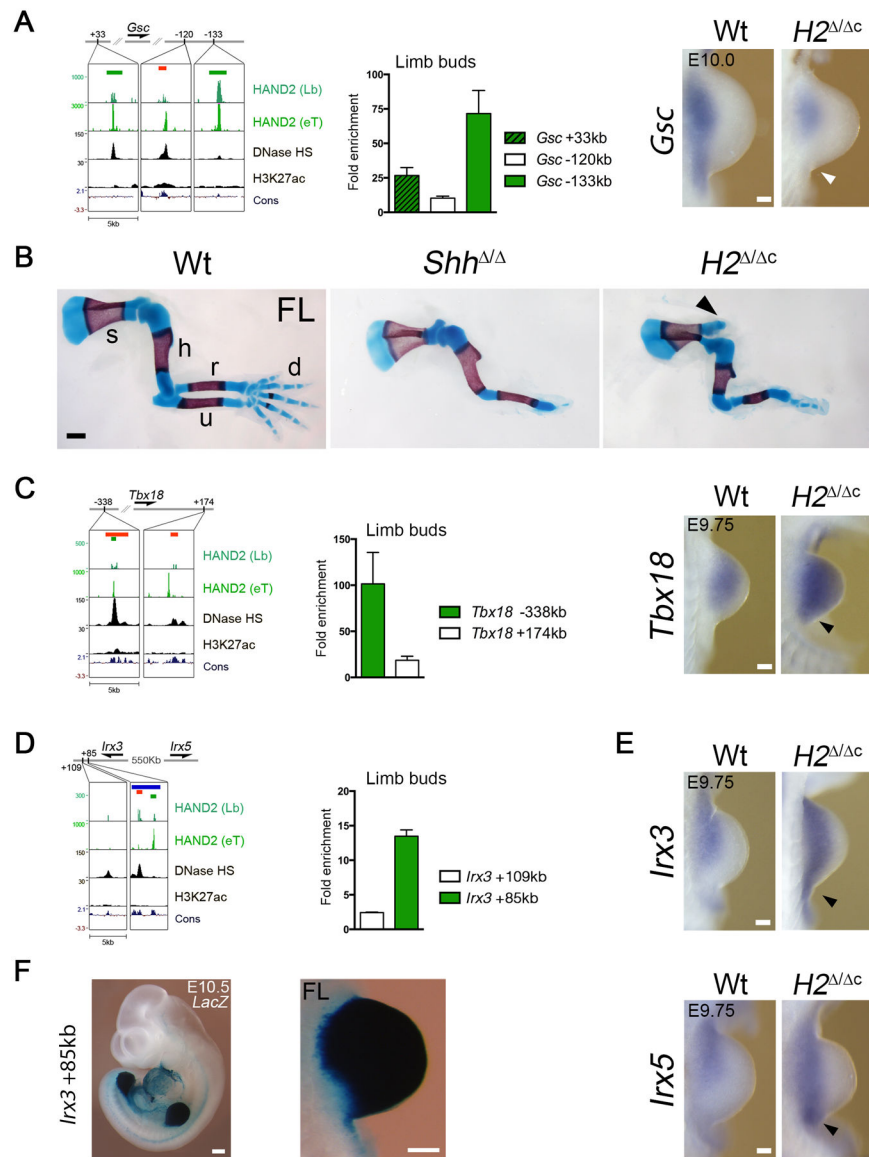
Figure 3. HAND2 directly regulates genes participating in proximal limb bud development

(A, C, D) HAND2^{3xF} ChIP profiles in the genomic landscapes encoding the *Gsc* (A), *Tbx18* (C) and *Irx3* (D) transcriptional regulators (left panels). Green bars: HAND2 ChIP-Seq peaks identified by MACS analysis. Red bars: genomic regions interacting with GLI3R in limb buds (Vokes et al., 2008). Blue bar: genomic region tested for enhancer activity in mouse transgenic embryos. Middle panels: ChIP-qPCR analysis to establish the significant enrichment of particular HAND2^{3xF} binding peaks in limb buds (E10.5). Mean ±SD (n=3). Right panels in (A) and (C): RNA *in situ* hybridization analysis of wild-type and *Hand2*$^{Δ/Δc}$ forelimb buds (E9.75, 28-29 somites; E10.0 30-31 somites). Black arrowheads: expanded expression domains. White arrowhead: reduction/loss of expression. Scale bars: 100μm. (B) Forelimb skeletons (FL) at E16.5 with cartilage in blue and bone in red. Arrowhead points to the malformed scapular head. s : scapula; h: humerus; r : radius; u : ulna; d : digits. Scale bar: 500μm.

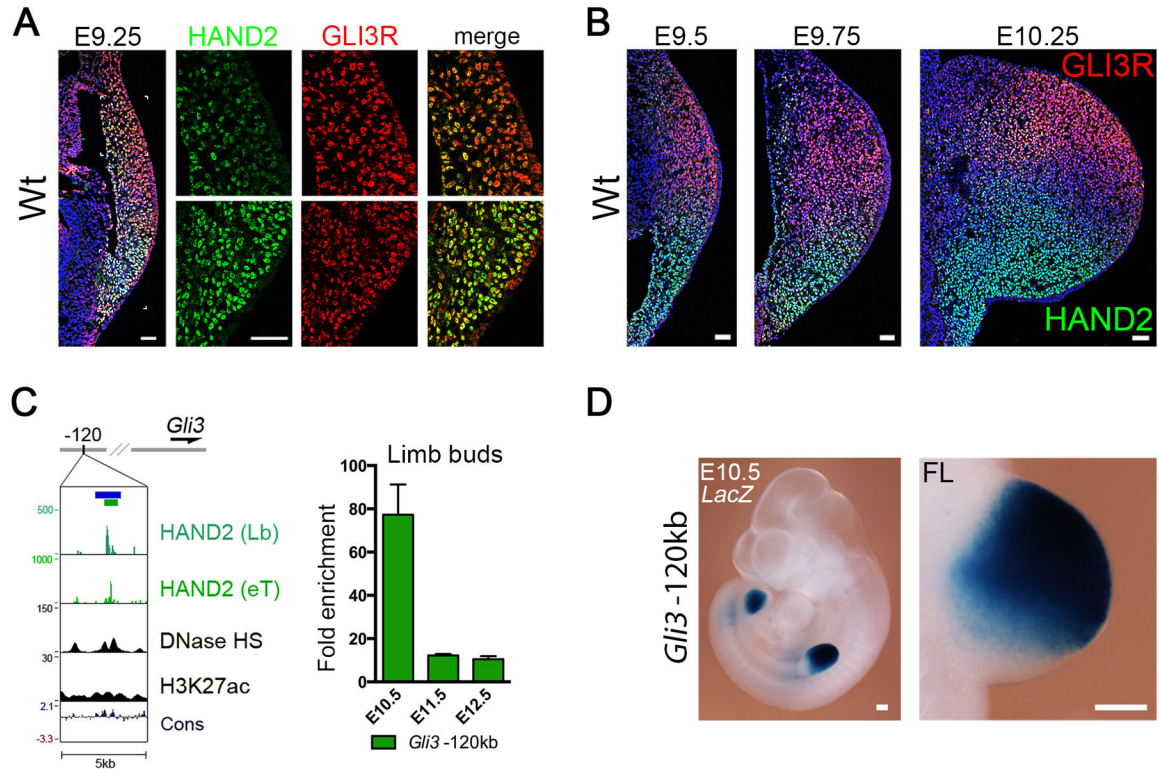(E) *Irx3* and *Irx5* expression in wild-type and *Hand2* $^{\Delta/c}$ forelimb buds (E9.75,28-29 somites)

(F) Expression of the *LacZ* reporter under control of the *Irx3* +85kb CRM in a transgenic embryos (E10.5) FL: forelimb bud. Scale bars: 200μm. See also Figure S3.

Figure 4. The dynamics of the HAND2 and GLI3R distributions reveal the establishment of a posterior and anterior limb bud compartment

(A, B) Co-immunolocalization of HAND2^{3xF} (green) and GLI3R (red) in wild-type forelimb buds at E9.25 (22-23 somites), E9.5 (25-26 somites), E9.75 (28-29 somites) and E10.25 (32-33 somites). Scale bars: 50μm.

(C) HAND2^{3xF} binding regions in the *Gli3* genomic landscape revealed by ChIP-Seq analysis (green). Blue bar demarcates the *Gli3* -120kb region chosen for *LacZ* reporter analysis. The right panel shows the temporal occupancy of the *Gli3* -120kb region by HAND2 complexes as revealed by ChIP-qPCR analysis of limb buds from E10.5-E12.5. Mean ±SD is indicated (n=3).

(D) Expression of the *LacZ* reporter under control of the *Gli3* -120kb HAND2 binding region in a transgenic embryo (E10.5) FL: forelimb bud. Scale bars: 200μm. See also Figures S4 and S5.
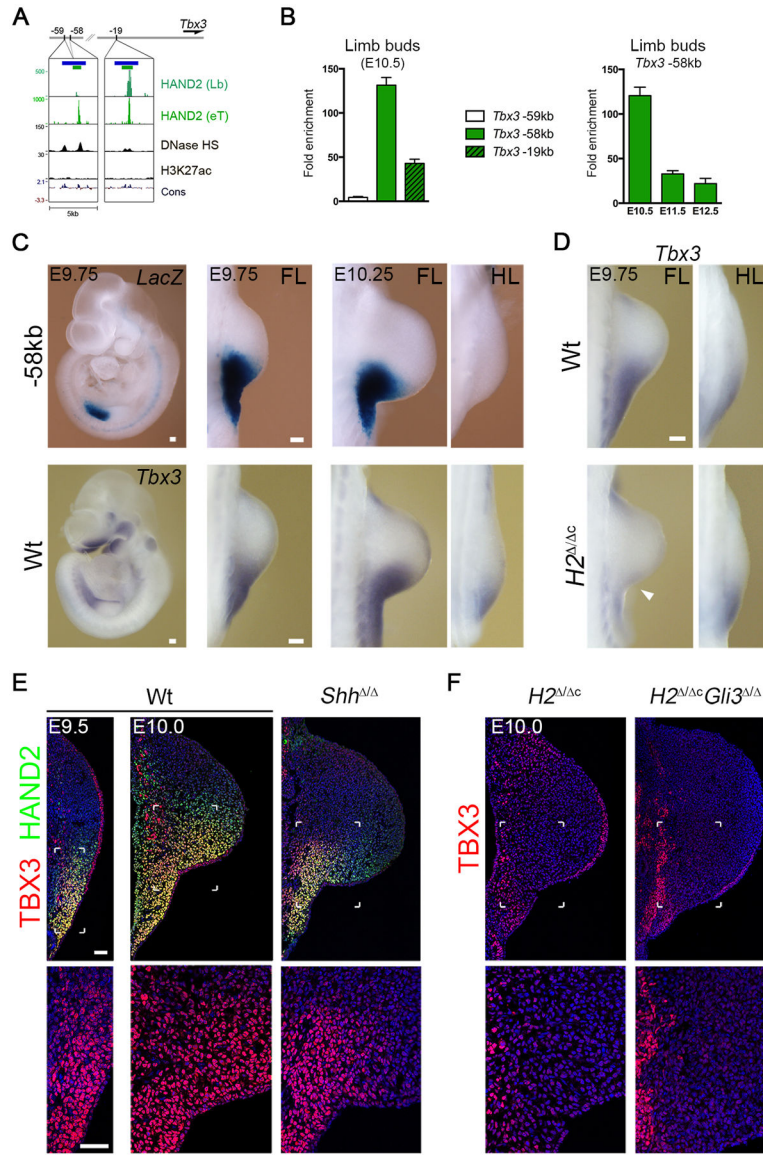
Figure 5. HAND2 controls *Tbx3* expression by interacting with a CRM that is active early in the posterior forelimb bud mesenchyme

(A) HAND2[3xF] binding regions in the *Tbx3* locus as defined by ChIP-Seq analysis.

(B) Left panel: ChIP-qPCR reveals the significance of the interactions of HAND2[3xF] chromatin complexes with the *Tbx3* -58kb and *Tbx3* -19kb regions in limb buds (E10.5). Mean ±SD (n=3). Right panel: temporal dynamics of the occupancy of the *Tbx3* -58kb region by HAND2[3xF] complexes in limb buds.

(C) Upper panels: Expression of *LacZ* under control of the *Tbx3* -58kb HAND2 binding region in transgenic embryos at E9.75 and E10.25. Lower panels: endogenous *Tbx3* transcript distribution in wild-type embryos. FL: forelimb bud, HL: hindlimb bud. Scale bars: 100μm.

(D) *Tbx3* expression in wild-type and *Hand2*[Δ/Δc] fore- (FL) and hindlimb (HL) buds at E9.75. White arrowhead: loss of *Tbx3* in the posterior forelimb bud mesenchyme. Scale bar: 100μm.

(E) Co-localization of the nuclear HAND2^{3xF} (green) and TBX3 (red) proteins in wild-type and *Shh*-deficient forelimb buds (E9.5, 25-26 somites and E10.0,30-31 somites). Lower panels show enlargements of the posterior TBX3 protein domains.

(F) TBX3 protein distribution in *Hand2*$^{\Delta/c}$ and *Hand2*$^{\Delta/c}$ *Gli3*$^{\Delta/\Delta}$ forelimb buds(E10.0, 30-31 somites). See also Figure S6.
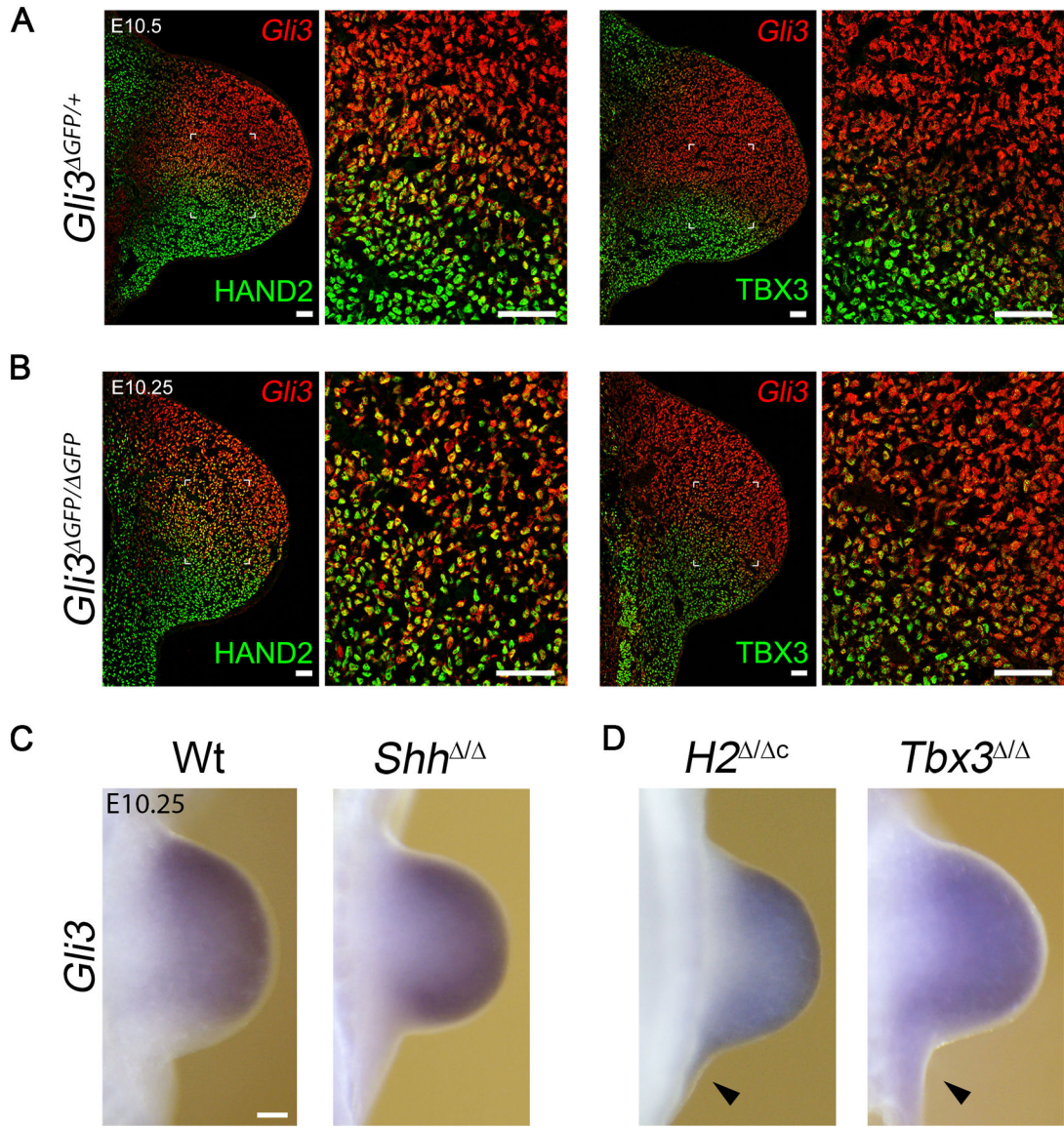
Figure 6. The TBX3 transcriptional repressor participates in excluding *Gli3* from the posterior limb bud mesenchyme

(A, B) Left panels: co-localization of HAND2^{3xF} proteins (green) with *Gli3* transcripts (red) in *Gli3*$^{\Delta GFP/+}$ (E10.5, 35-36 somites) and *Gli3*-deficient (*Gli3*$^{\Delta GFP/\Delta GFP}$; E10.25, 32-33 somites) forelimb buds. Right panels: co-localization of TBX3 proteins (green) with *Gli3* transcripts (red) in forelimb buds of the same genotypes. White marks indicate the enlargements. Cells co-expressing HAND2^{3xF} or TBX3 proteins with *Gli3* transcripts appear yellow. Scale bar: 50μm.

(C, D) *Gli3* transcript distribution in wild-type, *Shh*-deficient, *Hand2*$^{\Delta/\Delta c}$ and *Tbx3*$^{\Delta/\Delta}$ forelimb buds (E10.25; 32-33 somites). Arrowheads point to expanded *Gli3* expression in the posterior flank mesenchyme. Scale bar: 100μm. See also Figure S7.
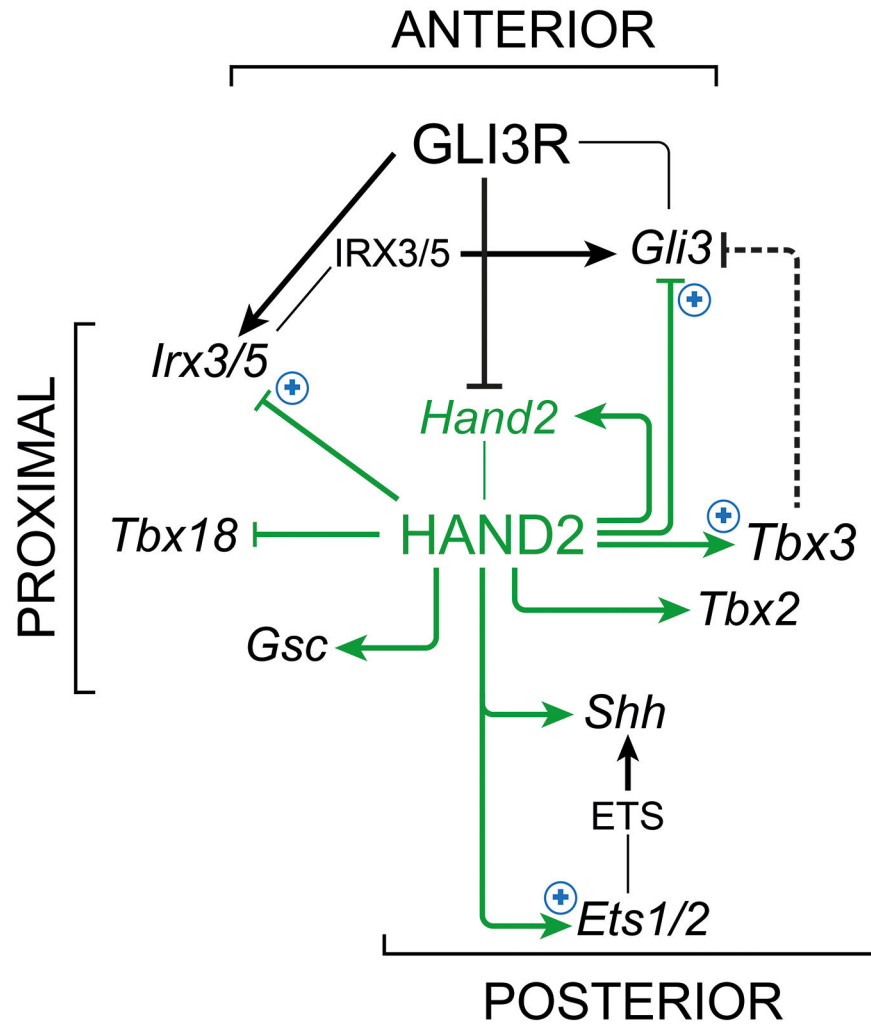
Figure 7. The major transcriptional interactions and networks governed by HAND2 in the forelimb bud mesenchyme upstream of SHH

HAND2 is at the core of the transcriptional networks that control establishment of a proximal, anterior and posterior compartment in early forelimb buds. In addition to directly impacting on *Shh* and *Gli3* expression, HAND2 re-enforces their activation and repression via *Ets1/2* and *Tbx3*, respectively. Solid lines indicate direct interactions, while dashed lines indicate interactions deduced from genetic analysis. Note that the activating or repressive nature of the interactions has mostly been deduced from genetic analysis. (+) indicates CRMs interacting with HAND2 chromatin complexes that have been identified in this study and drive *LacZ* reporter expression in the forelimb bud mesenchyme.

Table 1

Summary of the RNA *in situ* hybridization analysis of a select set of HAND2 target genes in *Hand2*-deficient limb buds

Validated ChIP-Seq peaks associated with genes encoding transcriptional regulators and/or essential roles during the onset of mouse limb bud development were selected. This table summarizes the alterations in their expression in *Hand2*-deficient mouse forelimb buds (E10.5). Genomic landscapes associated with genes functioning during progression of limb bud development, expressed in the limb bud ectoderm or at late stages (e.g. during chondrogenesis) were not considered for this study.

Gene	Down-regulated	Up-regulated	Not changed
Alx4[a]		■	
Bmp4[a]			■
Bmp7			■
Cyp26b1			■
Ets1	■		
Ets2	■		
Fgfr1			■
Furin	■		
Gas1		■	
Gli2			■
Gli3		■	
Gsc	■		
Irx3		■	
Irx5		■	
Lmx1b			■
Meis2			■
Msx1			■
Msx2[a]		■	
Mycn			■
Shh[b]	■		
Slit3	■		
Snai1			■
Tbx2	■		
Tbx3	■		
Tbx4			■
Tbx5			■
Tbx18		■	
Unc5c	■		
Zfp503	■		

[a]Genes analyzed by Galli et al. (2010).

*b*Only enriched in the eT ChIp-Seq dataset.